

Reverse draining of a magnetic soap film

D. E. Moulton*

Department of Mathematics, University of Arizona, Tucson, Arizona 85721, USA

J. A. Pelesko†

Department of Mathematical Sciences, University of Delaware, Newark, Delaware 19716, USA

(Received 20 January 2010; revised manuscript received 30 March 2010; published 30 April 2010)

We investigate the draining of a vertical magnetic soap film in the presence of a strong, nonuniform magnetic field. A colloidal suspension of magnetic nanoparticles in a regular soap solution yields a magnetic soap solution, from which a soap film is formed across an isolated frame. Experiments demonstrate that with a strong magnet placed above the frame, the film may be made to flow upward against gravity. The amount of film draining upward is altered by varying the distance between the frame and magnet. A first mathematical model is developed for the evolution of the film. Simulations demonstrate qualitative agreement with the experiment.

DOI: [10.1103/PhysRevE.81.046320](https://doi.org/10.1103/PhysRevE.81.046320)

PACS number(s): 47.65.Cb, 47.15.gm, 83.80.Hj, 68.15.+e

I. INTRODUCTION

The draining of a vertical soap film is a classic experiment in fluid mechanics due to both its experimental simplicity and the complexity of the mechanisms underlying it. Explored since the time of Newton [1], the first comprehensive study of draining films was performed by Mysels *et al.* [2]. They investigated a number of interesting features, including the formation of very thin film, termed “black film” at the top of the film, and a process they termed “marginal regeneration” which occurs at film boundaries and leads to the creation of black film.

The dynamics of a draining film are governed by a combination of viscous, capillary, and gravitational forces, along with surface tension effects and interactions with the film boundary. Drainage of thin films plays an important role in a number of industrial processes, most notably in the production of foams [3,4]. Numerous studies have been conducted and mathematical models proposed to understand the mechanics of draining and the roles of the different forces involved (e.g., [5–8]). One way to understand the physical properties of soap films is to add a controllable component to the system. This idea has been explored by Elias *et al.* [9], who added an aqueous suspension of magnetic nanoparticles to an ordinary soap solution, thus forming a magnetic soap solution. In other words, they replaced the continuous liquid phase of the soap solution with a ferrofluid or magnetic liquid. This added magnetic dimension was treated as a macroscopic force which could be controlled by subjecting the film to varying magnetic fields. In different studies, they used this idea to investigate the properties of magnetic cells [10] and foams [11]. More relevant to the present study, in one set of experiments [9], they subjected a vertical film draining into a bath to a uniform magnetic field and found that they could speed up or slow down the draining process based on the orientation of the magnetic field. In this paper, we explore a

similar experimental setup, but with a key difference: we place strong magnets above an isolated film, thus achieving much stronger and *nonuniform* magnetic fields. Magnetic particles experience a force in a nonuniform magnetic field; this phenomenon is known as magnetophoresis [12,13]. Thus, the nonuniformity of the field results in a body force acting on the film that is opposed to gravity, a force which is not present in a uniform field. When the magnetic field is strong enough, the fluid in the vertical film can be made to flow upward against gravity. This is a phenomenon in soap films which we term “reverse draining,” and which as far as we know has not been previously reported.

The present work lies at the intersection of two fields: the draining of films and ferrofluids. To our knowledge, the paper by Elias *et al.* [9], the present paper, and a companion paper which analyzes the model we derive here [14] are the only studies of this type. As mentioned above, one benefit of exploring this area is to better understand the process of a draining film. On the other hand, in the context of ferrofluids, magnetophoresis and the use of nonuniform magnetic fields with ferrofluids are connected to the idea of *controlling ferrofluids*. While the instability of ferrofluids has long been recognized [15] and pattern formation continues to be studied [16,17], interest in having direct control of the flow of a magnetic liquid has become quite substantial in recent years, largely due to possible applications in drug delivery and bioseparation (e.g., [18–20]). Even though such bioapplications have little direct connection to soap film, simple experiments with magnetic soap films may provide information not just on the properties of the soap films and foams, but also on the controllability of the ferrofluid as well.

In Sec. II, we present experimental results of the draining magnetic film. We demonstrate the phenomenon of reverse draining and explore the effect of changing the distance between the film and the magnet. In Sec. III, we suggest a simple mathematical model for the draining magnetic film, derived from first principles. Simulations demonstrate the basic effect and possible improvements for a more complete model are discussed.

*Corresponding author; moulton@math.arizona.edu

†pelesko@math.udel.edu

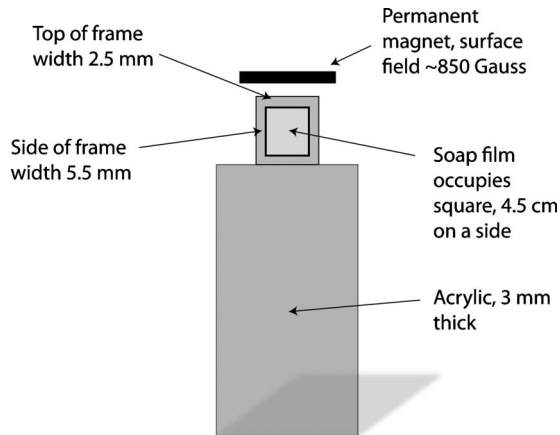


FIG. 1. Sketch of the experimental setup. The frame was lit using a standard fluorescent light and all photographs were captured using a Pixelink video camera with 1024×768 resolution at 20 frames per second.

II. EXPERIMENT

A. Magnetic soap film

The magnetic soap solution used here is created from a combination of a concentrated aqueous suspension of colloidal magnetic nanoparticles and an ordinary soap “bubble” solution. In particular, the soap bubble solution consists of 12 parts distilled water, one part commercial dish soap [26], and one part glycerin. The nanoparticle solution consists of a uniform colloidal suspension of 10 nm iron oxide (Fe_3O_4) particles at 4% concentration [27]. The soap solution and nanoparticle solution are mixed in a 2:1 ratio.

B. Experimental setup

The experimental setup is sketched in Fig. 1. The frame is swabbed with the magnetic soap solution to create the film. Immediately after, the magnet is slid in place directly above the frame, with the frame centered below the magnet. In all experiments, the same magnets were used so that the strength of the magnetic field is a constant. In order to vary the effect of the field, the distance between the frame and the magnet is varied.

C. Experimental results

The magnetic soap film consists of two outer layers of surfactant with an inner layer of ferrofluid. In the presence of an external magnetic field, the magnetic particles in the ferrofluid tend to align their dipoles with the direction of the field. The magnetization is paramagnetic—that is in the same direction as the applied field. With a strong magnetic field in place above the film, the magnetic nanoparticles feel an attraction toward the magnet which varies nonlinearly with distance from the magnet. Since the magnetic particles are many times larger than the water particles, they have the ability to drag fluid with them as they move toward the magnet. Thus, close to the magnet, the film can drain upward if the magnet is strong enough. At a large-enough distance, the gravitational force is stronger and the fluid flows downward.

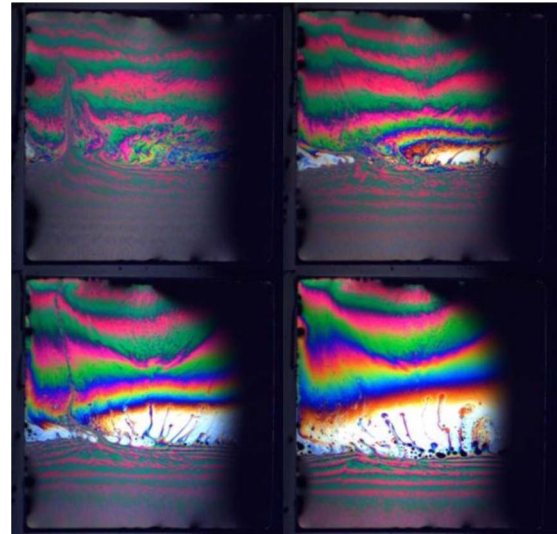


FIG. 2. (Color online) Sequence of pictures, 7 s apart, showing the process of reverse draining for a film with a gap distance of 2.5 mm between the film and magnet. The thin region is marked by the white strip which appears in the middle of the film and grows over time.

Figure 2 shows a sequence of a draining film at a distance of 2.5 mm between film and magnet (i.e., just the width of the frame). The first picture was taken 3 s after the magnet was put in place and 7 s elapse between each picture. The white and silver portions of the film mark thin regions, while the black spots are the so-called black film and are the thinnest regions. At this gap distance, the film begins to thin about two thirds of the way down the film. Below the thin strip, gravity is stronger than the magnetic force and the film drains downwards; above the thin region, the magnetic force is stronger and the fluid flows upward. In this sense, the white strip can be seen as a boundary between the two opposing vertical forces. As time increases, the thin region grows. However, the draining film was not very stable—most likely due to evaporation and the leakage of soap solution across the top and bottom of the frame—and so not long after the formation of the thin region the film would rupture. The total time elapsed between the formation of the film and its rupture was on the order of 30 s.

Observe that although there is variation across the film, the color bands are close to being horizontal. Horizontal variation will be caused by surface tension gradients, turbulence induced by side boundary interactions [21], as well as by horizontal components of the magnetic field. Notice also that the color bands are more regular and horizontal below the thin region, where the magnetic field has small effect. This suggests that it is the magnetic field that is responsible for the majority of the variation. Nevertheless, that the film is close to being uniform in the horizontal direction suggests that, to a first approximation, forces act primarily in the vertical direction. We will utilize this assumption in deriving a model in Sec. III.

The effect of the distance between film and magnet is demonstrated in Figs. 3 and 4. As the distance between the film and magnet is increased, the strength of the magnetic

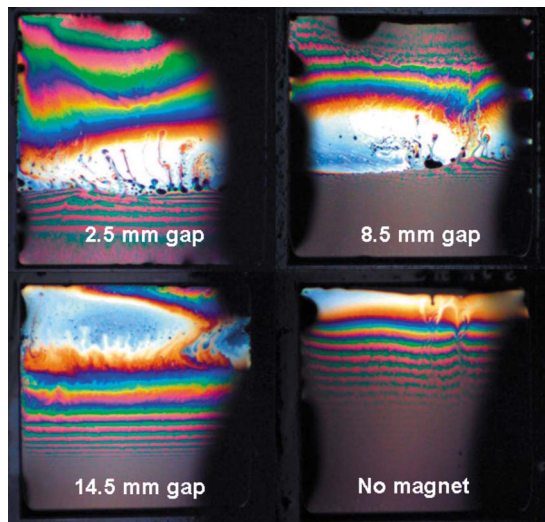


FIG. 3. (Color online) Snapshot of the draining film right before rupture for gap distances of 2.5, 8.5, and 14.5 mm, as well as a control case with no magnet.

field is effectively weakened and the boundary between the vertical body forces of gravity and the magnetic force is moved to a higher point on the film. Thus the location at which the film thins occurs at a higher point. Figure 3 shows snapshots of the film right before rupture for distances of 2.5, 8.5, and 14.5 mm. At a gap of 14.5 mm, the magnetic field has a relatively weak effect—there is only a thin strip of fluid above the thin region. For comparison, we also include a picture in the case where the magnet is absent. Here, drainage is purely downward and the film thins at the very top of the frame.

In Fig. 4, the average location of the thin white region over several trials is plotted against the three gap distances of 2.5, 8.5, and 14.5 mm. In each trial, upper and lower boundaries are marked right before rupture. In Fig. 4, the frame length is normalized to unity, so that the top of the frame

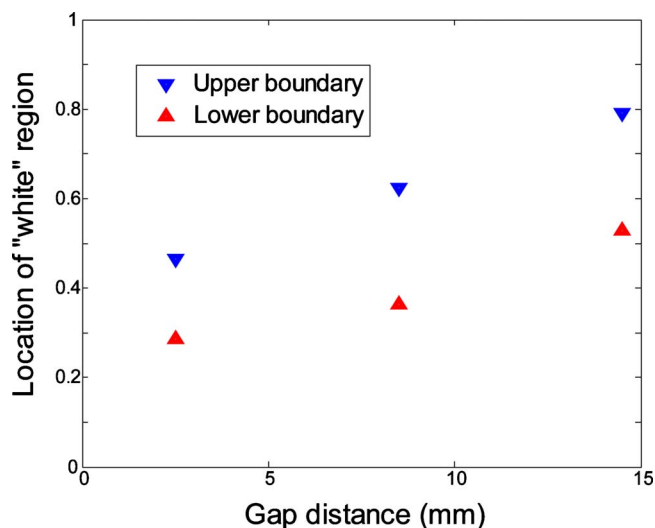


FIG. 4. (Color online) Location of the thin white region as a function of gap distance. Average values for the upper and lower boundaries of the white strip are averaged over trials.

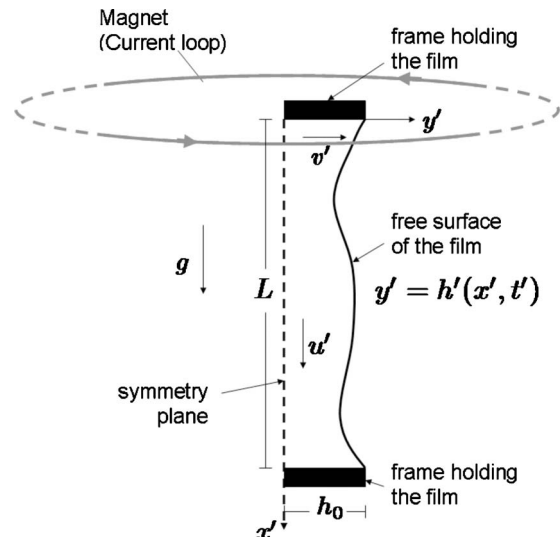


FIG. 5. Setup for the draining magnetic film system on which the model is based.

corresponds to 1 and the bottom of the frame to zero. As the distance is increased, the size of the white region increases slightly and its location moves up the frame.

There are several features of the experiment that we have not presented. One intriguing aspect is the motion of the black film patches that are created at film boundaries. Preliminary experiments suggest that these patches can move downward in the presence of a strong magnet, contrary to the conventional understanding that they always move upward as a buoyancy effect [2]. Also, experiments conducted using a cylindrical soap film and a different soap solution led to a stable configuration of black film being reached. It was then found that the location of the black film could be well controlled by moving the magnet. We mention these observations as suggestions for future investigation only, as our intention here is to introduce the basic experiment and the phenomenon of reverse draining.

III. MATHEMATICAL MODEL

In this section, we propose a first model for the draining of a magnetic soap film in the presence of a nonuniform magnetic field. The setup is depicted in Fig. 5. Using primes to denote dimensional variables, the film is described by the function $y' = h'(x', t')$, which is the half thickness of the film, assuming symmetry about the center line. The full film is envisioned by extending the profile in the transverse z' direction—that is, the film is a sheet independent of z' and with reflectional symmetry about $y' = 0$. Depending on film recipe, in particular surfactant concentrations, the surface of a draining soap film may be rigid or tangentially immobile. This is the assumption we make for this model, although simulations using a surface slug flow assumption as utilized in [6], did not drastically alter the behavior. Letting $\mathbf{u}' = (u', v')$ be the velocity vector of the fluid and starting from the Navier-Stokes equations, the fluid satisfies

$$\nabla \cdot \mathbf{u}' = 0,$$

$$\rho \left(\frac{\partial \mathbf{u}'}{\partial t} + \mathbf{u}' \cdot \nabla \mathbf{u}' \right) = \mu \nabla^2 \mathbf{u}' - \nabla p' + \rho g \hat{x} + \mu_0 (\mathbf{M}' \cdot \nabla) \mathbf{H}'. \quad (1)$$

Here, ρ is fluid density, p' is pressure, g is the gravitational constant, and μ is the dynamic viscosity. The term $\mu_0 (\mathbf{M}' \cdot \nabla) \mathbf{H}'$ is the added body force due to the nonuniform magnetic field, assuming the solution is a dilute colloidal solution of magnetic particles [22]. Here, μ_0 is the magnetic permeability of free space. The ferrofluid is paramagnetic, so that the magnetization $\mathbf{M}' = (\mathbf{M}'_1, \mathbf{M}'_2)$ is aligned with the applied field $\mathbf{H}' = (\mathbf{H}'_1, \mathbf{H}'_2)$. We assume that we have a linear media, so that $\mathbf{M}' = \chi_m \mathbf{H}'$, where χ_m is the susceptibility constant.

Along the symmetry plane of the film $y'=0$, we require

$$\frac{\partial u'}{\partial y} = 0, \quad v' = 0 \quad (2)$$

and at the free surface $y'=h'(x',t')$, we have

$$\frac{\partial h'}{\partial t'} = v' - u' \frac{\partial h'}{\partial x'},$$

$$[\hat{\mathbf{n}} \cdot \mathbf{T} \cdot \hat{\mathbf{n}}] = \gamma \bar{H},$$

$$u' = 0. \quad (3)$$

Here, $\hat{\mathbf{n}}$ is the unit normal vector, \mathbf{T} is the stress tensor, γ is the surface tension of the film-air interface, and \bar{H} is the mean curvature of the free surface. These conditions are the kinematic condition, normal stress balance, and tangentially immobile requirement, respectively.

A. Lubrication theory

Let $L = (\gamma/\rho g)^{1/2}$ be a characteristic length scale in the vertical direction, chosen to balance surface tension with gravity, and h_0 a characteristic length in the horizontal direction. For the present material, $L=2$ mm and we take $h_0 = 10 \mu\text{m}$. Then $\epsilon = h_0/L$ is a small parameter. To carry out lubrication theory, vertical lengths are scaled by L and horizontal lengths by h_0 . The vertical velocity component is scaled by $U_0 = \rho g h_0^2 / \mu$ and the horizontal component by ϵU_0 . Time is nondimensionalized by L/U_0 and pressure is scaled by $\mu L U_0 / h_0^2$. For the magnetic terms, we scale the vertical magnetic component H'_1 by H_0 , a characteristic value for the applied field. As the film is very thin, H_1 is assumed to be a function only of x to first order. Also, since the magnetic field is primarily vertical, the horizontal component H_2 is scaled by ϵH_0 . To leading order, the scaled equations are

$$\begin{aligned} u_x + v_y &= 0, \\ u_{yy} - p_x + 1 + \lambda H_1 H_{1x} &= 0 \\ -p_y &= 0. \end{aligned} \quad (4)$$

Here,

$$\lambda = \frac{\mu_0 \chi_m H_0^2}{\rho g L} \quad (5)$$

is a dimensionless parameter characterizing the strength of the magnetic field. The boundary conditions at $y=0$ become

$$u_y = 0, \quad v = 0. \quad (6)$$

At the free surface $y=h(x,t)$, the condition of tangential immobility is $u=0$ and the kinematic condition is

$$h_t = v - u h_x. \quad (7)$$

Combined with the first equation of (4), this may be written as

$$h_t + \int_0^h u dy = 0. \quad (8)$$

Integrating the second equation of Eq. (4) and using the boundary conditions (6) and tangential immobility, we can solve for u . Plugging into Eq. (8), we obtain

$$h_t - \frac{\partial}{\partial x} \left(\frac{h^3}{3} (p_x - 1 - \lambda H_1 H_{1x}) \right) = 0. \quad (9)$$

The scaled normal stress condition is

$$p = -\sigma h_{xx}, \quad (10)$$

where $\sigma = \epsilon^3 / \text{Ca}$, with $\text{Ca} = \mu U_0 / \gamma$ the capillary number. Taking a derivative of Eq. (10) with respect to x , Eq. (9) becomes

$$h_t + \frac{\partial}{\partial x} \left(\frac{h^3}{3} (\sigma h_{xxx} + 1 + \lambda H_1 H_{1x}) \right) = 0. \quad (11)$$

Note that the term inside the x derivative is the velocity flux $Q(x,t)$ over a horizontal cross section; that is

$$Q(x,t) = \frac{h^3}{3} (\sigma h_{xxx} + 1 + \lambda H_1 H_{1x}).$$

To complete the system, boundary conditions are needed at the top and bottom of the film. Since the experiment consists of an isolated frame, the natural conditions to impose are that there is no flux of fluid across the frame and that the film thickness remains fixed at the frame. This is expressed as

$$\begin{aligned} h(0,t) &= h(\alpha,t) = h_b, \\ Q(0,t) &= Q(\alpha,t) = 0, \end{aligned} \quad (12)$$

where α is the ratio of the length of the frame to L and h_b is the ratio of the half thickness of the film at the ends to h_0 .

B. Magnetic field

Equation (11), along with boundary conditions (12) and a given initial profile, describe the evolution of the free surface of the film under the combined effects of gravity, surface tension, viscosity, and an arbitrary magnetic field that is a function only of x to first order. To check the qualitative

behavior of the system, we model the magnet as a current loop (see Fig. 5) and suppose that the film is perfectly centered beneath the loop. Along the line which runs through the center of the current loop and is normal to the plane of the loop, the magnetic field only has a vertical component, which can be computed exactly [23]. For a loop of radius R and with current I , the magnetic field is $\mathbf{B}' = B' \hat{\mathbf{x}}$, with

$$B' = \frac{\mu_0 I R^2}{2(R^2 + x'^2)^{3/2}}. \quad (13)$$

Here, x' is the distance from the current loop. Equation (13) is exact along the vertical line through the center of the film, i.e., the symmetry line. Off of this line, the magnetic field is different and has both a vertical and a horizontal y' component. However, since the film is very thin, the field will not deviate much from Eq. (13) and so we assume that Eq. (13) describes the magnetic field throughout the film to first order.

This assumption becomes problematic when we add in the third dimension, the transverse z' direction or width of the frame. With a fully three-dimensional film, the magnetic field may have a significant z' component, unless the width of the frame is much smaller than the radius of the current loop or magnet. In a 3D model, a nonnegligible field component in the z' direction would not be problematic as far as deriving an evolution equation. The only necessity in carrying through lubrication theory is that the field does not have a significant y' component. Our purpose here is to derive a model with the simplest representation of the field which still captures the basic effect. Based on the results of our experiments, in particular, the fact that the films stayed nearly uniform horizontally, it seems a reasonable approximation to only treat the vertical component of the magnetic field.

Using the connection $\mathbf{B}' = \mu_0(\mathbf{H}' + \mathbf{M}')$, we obtain from Eq. (13) the vertical component H'_1 . Letting $H_0 = I[2R(1 + \chi_m)]^{-1}$, in dimensionless form we have

$$H_1 = (1 + \eta^2 x^2)^{-3/2}, \quad (14)$$

where $\eta := L/R$ relates the vertical length scale to the radius of the current loop. From this, the body force term $H_1 H_{1,x}$ is computed. Denoting this by $f(x)$, we have

$$f(x) := H_1 H_{1,x} = \frac{-3\eta^2 x}{(1 + \eta^2 x^2)^4}. \quad (15)$$

This derivation is for a film located directly below the current loop. To allow for a gap of distance d (dimensionless) between the film and current loop, let $x=0$ represent the top of the film. Then the current loop is located at $x=-d$ and we replace $f(x)$ with $f(x+d)$. Thus, the evolution equation for the draining magnetic film is

$$h_t + \frac{\partial}{\partial x} \left\{ \frac{h^3}{3} [\sigma h_{xxx} + 1 + \lambda f(x+d)] \right\} = 0. \quad (16)$$

This equation is accompanied by the boundary conditions (12) and an initial profile.

C. Sample calculations

Equation (16) is a fourth-order degenerate diffusion equation and is typical of evolution equations arising from the

TABLE I. Parameter values used in simulations.

Parameter	Value
g : acceleration of gravity	9.8 m/s ²
ρ : density of the solution	1.1 g/cm ³
γ : surface tension	0.042 N/m
μ : viscosity	2 cP
μ_0 : magnetic permeability	$4\pi 10^{-7}$ N/A ²
B_0 : magnetic field strength	1684 G
χ_m : magnetic susceptibility	0.05
R : radius of current loop	4.4 cm
h_b : film thickness at edge	1 mm

lubrication approximation. Numerous studies have analyzed the properties of these types of equations (for example, [24,25] and references therein). However, a key component present in the current model that is not found in most such models is the nonautonomous forcing function $f(x+d)$. The addition of this function both changes the film behavior and complicates standard techniques of analysis. A detailed analytical and numerical analysis of Eq. (16), as well as similar evolution equations with arbitrary nonuniform forcing, is given in a companion paper [14]. These systems possess a rich solution set, the complexity of which depends strongly on the properties of the external forcing.

The model we have derived is an attempt at capturing the added nonuniform and nonlinear magnetic effects of a draining film. Several physical components are missing from the model, including surfactant concentration and Marangoni effects, microscopic interactions between the magnetic particles, as well as complex interactions at the boundary of the film. Hence, a full quantitative comparison to experiment is not feasible at present. Rather, our intent is to consider the qualitative behavior of the model for reasonable parameter values and show that basic phenomena are captured.

Equation (16) along with boundary conditions (12) was solved numerically for parameters given in Table I and for the three tested distances between film and magnet, 2.5, 8.5, and 14.5 mm. Some of the parameters in the system are well known to us while others are less well known. The density, surface tension, and viscosity are easily measured and are typical of soap films. The film thickness at the edge, which plays a very important role in the time scale, is difficult to determine. We use the value of a 1-mm-thick film at the upper and lower boundaries. If this value is decreased by a factor of 10, the drainage slows down by a factor of about 1000. The magnetic parameters were also difficult to determine exactly. In particular, the magnetic field in the experiment is provided by multiple square magnets, whereas the model assumes a circular current loop. For simplicity, a flat initial profile was used, although simulations with a parabolic concave-in profile did not alter the evolution much. The system was solved using a conservative numerical scheme, second order in space and time. For details of the numerics, including convergence properties, see [14].

Figure 6(a) shows the evolution of the film for a 2.5 mm gap plotted in dimensional variables. As time progresses, the

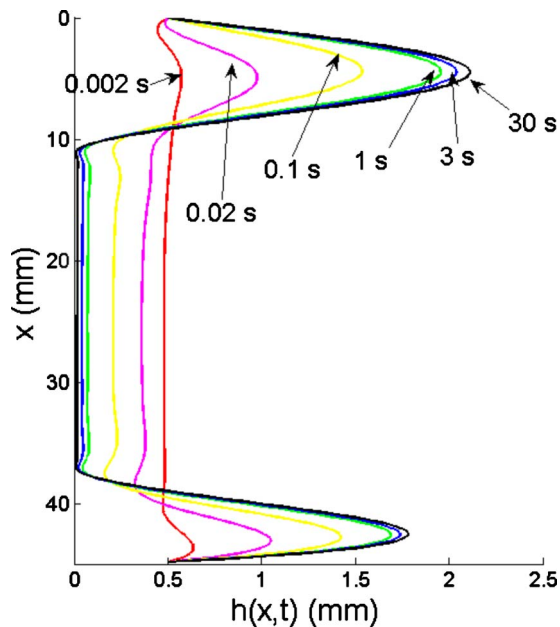


FIG. 6. (Color online) Evolution of the film for 2.5 mm gap. The times of the different profiles are indicated.

film thins in the middle, with fluid collecting at both the top and bottom, relating the competition between gravity and magnetic forces. The majority of fluid motions happen on a fast time scale—most of the drainage occur within the first couple seconds, after which the film approaches $h(x,t)=0$ in the thin region on a slower time scale. Comparing to Fig. 2, this is not inconsistent with the experiment—the thin region first appears after about 3 s and then slowly expands over the next tens of seconds.

Equation (16) along with boundary conditions (12) tends to an equilibrium profile as time goes to infinity [14]. Zooming in on the thin region demonstrates that the film continues to thin, never reaching $h=0$ in finite time. It is unclear whether this is the case in the experiments, as the film would tend to rupture before reaching an equilibrium state, most likely due to evaporation. Further, key to the equilibrium profile is the no flux boundary condition, which forces a volume constraint; consequently, the film approaches an equilibrium balance between the primary forces of gravity and the magnetic field. This no-flux condition is at best an approximation, alternate boundary conditions which allow flux across the boundary significantly alter the long-time film evolution (see [14]).

The effect of gap distance is seen in Fig. 7, where the film profile after 60 s is plotted for the three gap distances 2.5, 8.5, and 14.5 mm, as well as for the case of no magnet. As the gap distance is increased, the main observable effect is that a smaller volume of fluid drains upward and more fluid drains to the bottom of the film, indicating the reduced effective strength of the magnetic field with increased distance between magnet and film. Also, the upper boundary of the thin region moves up the film with increased gap while the lower boundary does not vary. Here, the model departs from experimental observation and Fig. 4, although again it is unclear how close the experiments were to an equilibrium state.

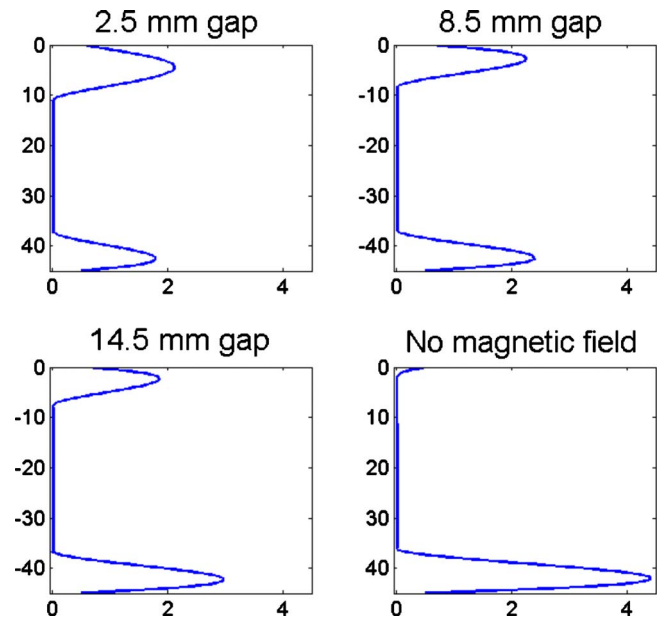


FIG. 7. (Color online) Equilibrium profiles for the three tested gap distances, as well as the case with no magnetic field. In each case, the solution profile is plotted at time 60 s. Both axes are in mm.

IV. SUMMARY AND EXTENSIONS

In this paper, we have investigated the drainage of a vertical magnetic soap film. Similar to a previous study [9], we have shown that control of the drainage may be achieved through application of a magnetic field. Here, though, we have demonstrated that by using strong, nonuniform fields, in fact the fluid may be made to drain upward against gravity in the phenomenon of reverse draining. The nonuniformity of the field created a competition between gravity and the magnetic force whereby gravity would be dominant on part of the film and the magnetic force dominant on another. This competitive “boundary” is tunable by altering the distance between film and magnet, although presumably a similar effect could be achieved by altering the strength of an electromagnet.

We have presented a basic model for the evolution of the free surface of the film. The model has exploited a number of simplifications in order to focus on the principal effect of the nonuniform magnetic field. Hence, it captures the mechanism of reverse draining, but is too simplified to reproduce the experiments in any quantitative fashion. Some additions in an improved model are relatively straightforward and so the present work might serve as a starting point to explore the process in more detail. Other additions provide a greater challenge, such as a more precise description of boundary interactions. An important addition which is poorly understood in the literature is the concentration of the magnetic particles.

The present study is preliminary, but suggests some interesting possibilities both broadly in the theory of fluid control for ferrofluids and specifically in the context of understanding draining soap films and marginal regeneration, a concept which is not entirely understood. An interesting area to ex-

plore in future investigations would be the use of more complex fields. For instance, the use of multiple magnets with differing orientations could yield intriguing draining patterns. A model for such a scenario would almost certainly need to be three dimensional, although the only fundamental

challenge with adding a third dimension to our model is capturing the magnetic field appropriately. Alternatively, keeping a simplified field and exploring different sizes and shapes of films could lead to a better understanding of the basic mechanisms of drainage.

-
- [1] I. Newton, *Opticks* (S. Smith & B. Walford, London, 1704).
- [2] K. J. Mysels, K. Shinoda, and S. Frankel, *Soap Films-Studies of Their Thinning and a Bibliography* (Pergamon Press, London, 1959).
- [3] A. J. Wilson, *Foams: Physics, Chemistry and Structure* (Springer-Verlag, London, 1989).
- [4] A. M. Kraynik, *Annu. Rev. Fluid Mech.* **20**, 325 (1988).
- [5] R. J. Braun, S. A. Snow, and U. C. Pernisz, *J. Colloid Interface Sci.* **219**, 225 (1999).
- [6] L. W. Schwartz and R. V. Roy, *J. Colloid Interface Sci.* **218**, 309 (1999).
- [7] V. A. Nierstrasz and G. Frens, *J. Colloid Interface Sci.* **215**, 28 (1999).
- [8] R. J. Braun, S. A. Snow, and S. Naire, *J. Eng. Math.* **43**, 281 (2002).
- [9] F. Elias, J.-C. Bacri, C. Flament, E. Janiaud, D. Talbot, W. Drenckhan, S. Hutzler, and D. Weaire, *Colloids Surf., A* **263**, 65 (2005).
- [10] F. Elias, I. Drikis, A. Cebers, C. Flament, and J.-C. Bacri, *Eur. Phys. J. B* **3**, 203 (1998).
- [11] F. Elias, C. Flament, J. A. Glazier, F. Graner, and Y. Jiang, *Philos. Mag. B* **79**, 729 (1999).
- [12] T. B. Jones, *Electromechanics of Particles* (Cambridge University Press, New York, 1995).
- [13] Y. Gao, Y. C. Jian, L. F. Zhang, and J. P. Huang, *J. Phys. Chem. C* **111**, 10785 (2007).
- [14] D. E. Moulton and J. Lega, *Physica D* **238**, 2153 (2009).
- [15] M. D. Cowley and R. E. Rosensweig, *J. Fluid Mech.* **30**, 671 (1967).
- [16] D. P. Jackson and J. A. Miranda, *Phys. Rev. E* **67**, 017301 (2003).
- [17] R. M. Oliveira, J. A. Miranda, and E. S. G. Leandro, *Phys. Rev. E* **77**, 016304 (2008).
- [18] C. H. Ahn, M. G. Allen, W. Trimmer, Y. N. Jun, and S. Er-ramilli, *J. Microelectromech. Syst.* **5**, 151 (1996).
- [19] E. P. Furlani, *J. Appl. Phys.* **99**, 024912 (2006).
- [20] H. D. Liu, W. Xu, S. G. Wang, and Z. J. Ke, *Appl. Math. Mech.* **29**, 1341 (2008).
- [21] H. N. Stein, *Adv. Colloid Interface Sci.* **34**, 175 (1991).
- [22] R. E. Rosensweig, *Ferrohydrodynamics* (Cambridge University Press, New York, 1985).
- [23] D. J. Griffiths, *Introduction to Electrodynamics*, 3rd ed. (Prentice Hall, New Jersey, 1999).
- [24] A. L. Bertozzi and M. Pugh, *Commun. Pure Appl. Math.* **49**, 85 (1996).
- [25] R. S. Laugesen and M. C. Pugh, *Eur. J. Appl. Math.* **11**, 293 (2000).
- [26] Dawn™ was used.
- [27] Solution EMG 705 obtained from Ferrotec Corporation.